

Short-range structure of simulated colloidal aggregates

Geoffrey C. Ansell and Eric Dickinson*

Procter Department of Food Science, University of Leeds, Leeds LS29JT, United Kingdom

(Received 6 November 1986)

The effect of colloidal interactions on the structure of aggregates formed by irreversible diffusion-controlled aggregation is studied by Brownian dynamics simulation. Three-dimensional systems of spherical particles with Derjaguin-Landau-Verwey-Overbeek (DLVO) pair potentials are simulated at various volume fractions. We find that the form of DLVO potential affects short-range structure as measured by the particle-particle correlation function, but not long-range structure as measured by the fractal dimension.

It is now established^{1,2} that the short-range liquidlike structure in a stable colloidal dispersion is dependent on the nature of the interactions between the particles. It seems plausible, therefore, to speculate that the short-range structure in an aggregate formed by irreversible diffusion-controlled coagulation might be sensitive to the nature of the interactions (attractive and repulsive) which were acting between the particles immediately prior to their sticking together.

Computer simulation^{3,4} and experiments with silica and gold colloids^{5,6} have shown that the stringy aggregates produced by Brownian coagulation are fractal in structure when examined on length scales much larger than the sizes of individual particles. General fractal scaling behavior is relatively insensitive to the chemistry of the colloidal system, or to details of the simulation model.⁷ On a length scale of a few particle radii, however, we do not expect such universality. Indeed, recent small-angle x-ray scattering measurements have demonstrated^{8,9} that aggregate structure is nonfractal on such a short-length scale. At large values of the pair separation r , the particle-particle correlation function $g(r)$ scales as r^{D-3} , where D is the fractal dimension. But, at short separations, we might expect to see more detailed features in $g(r)$: (i) geometrical packing constraints due to particle impenetrability (repulsive forces), and (ii) nonbonded particle clustering associated with reversible flocculation (attractive forces). From experience of $g(r)$ in stable colloids,^{1,2} one might expect short-range structure in aggregates to become more enhanced with increasing particle volume fraction.

The two pair potentials of mean force $U(r)$ chosen for study here are shown in Fig. 1. Both potentials are *strongly* attractive at close surface-to-surface separations ($r \rightarrow 2a$, where a is the particle radius), thereby implying irreversible aggregation on contact. Both potentials are *weakly* attractive at moderately large surface-to-surface separations ($r \sim 3a$), thereby implying a tendency to aggregate even in the absence of Brownian motion. Curve *A* differs from curve *B*, however, in having a repulsive region at intermediate separations ($2.15 \lesssim r/a \lesssim 2.3$). The turning points of maximum and minimum potential energy U in curve *A* are usually called the primary maximum and secondary minimum, respectively. The effect of the secondary minimum is to cause pairs of particles to associate loosely at separations $r \approx 2.3a$, before thermal motion ei-

ther induces dissociation or causes irreversible aggregation into the primary minimum ($r \rightarrow 2a$) after jumping over the primary maximum.

Physically, potentials of the types *A* or *B* in Fig. 1 are found¹ in some electrostatically stabilized colloidal dispersions to which a controlled amount of salt has been added. The algebraic forms of these Derjaguin-Landau-Verwey-Overbeek (DLVO) potentials¹⁰ are given by

$$U(r) = U_R(r) + U_A(r), \quad (1)$$

where $U_R(r)$ is a screened Coulombic repulsion and $U_A(r)$ is the van der Waals attraction. Under conditions where additivity of DLVO potentials is a valid concept ($\kappa a \gg 1$), $U_R(r)$ has the form¹⁰

$$U_R(r) = 2\pi\epsilon_r\epsilon_0a\psi_0^2 \ln[1 + \exp(-\kappa s)], \quad (2)$$

where $s = r - 2a$ is the surface-to-surface separation, ϵ_r is the relative dielectric constant of the medium, ϵ_0 is the permittivity of free space, ψ_0 is the particle surface potential, and κ is the inverse Debye length defined for a 1:1 electrolyte by

$$\kappa^2 = 2e^2CN_A/\epsilon_r\epsilon_0k_B T, \quad (3)$$

where e is the electronic charge, N_A is Avogadro's number, k_B is Boltzmann's constant, T is the absolute temperature, and C is the electrolyte concentration. The unretarded van

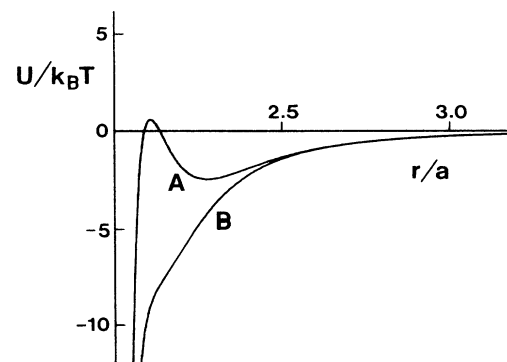


FIG. 1. The DLVO potentials *A* and *B*. Energy U is plotted against center-to-center separation r .

der Waals interaction has the form¹¹

$$U_A(r) = -(A/12)\{[4a^2/(r^2 - 4a^2)] + (2a/r)^2 + 2\ln[1 - (2a/r)^2]\}, \quad (4)$$

where A is the effective Hamaker constant. Parameter values are set as follows: $a = 0.25 \mu\text{m}$, $\epsilon_r = 80$, $T = 300 \text{ K}$, $\psi_0 = 20 \text{ mV}$, $A = 1.94 \times 10^{-19} \text{ J}$, $C(A) = 0.3 \text{ mol m}^{-3}$, $C(B) = 0.6 \text{ mol m}^{-3}$.

To represent short-range structure realistically in a system of spherical particles requires the use of a nonlattice simulation model. Our model consists here of 512 DLVO particles executing three-dimensional Brownian motion in a cubic cell with periodic boundary conditions. Translational diffusive motion of particles and aggregates is simulated using a Brownian dynamics algorithm¹²⁻¹⁴ based on the Langevin equation; inertial terms are neglected, but interparticle direct forces and hydrodynamic interactions are incorporated. The simulation time step was set in the range 2.5–20 μs . The scalar diffusion coefficient D_N of an N -particle aggregate is assumed to be given by

$$D_N = (k_B T / 6\pi\eta a) N^\gamma, \quad (5)$$

where η is the viscosity of the medium (water at 300 K), and γ is a hydrodynamic scaling coefficient with a value of -0.54 for fractal aggregates produced by cluster-cluster simulation.¹⁵ Strictly speaking, the use of Eq. (5) involves an *a priori* assumption about the fractal character of the aggregates to be formed during the simulation (since D_N properly scales as $N^{-1/D}$),¹⁶ and indeed the aggregates formed turn out to be rather more compact than implied by $\gamma = -0.54$. Although it does have a slight effect on the coagulation kinetics, especially in the later stages, we do not believe, however, that the exact choice of γ in Eq. (5) has any significant effect on the structural conclusions drawn below. (It has been shown elsewhere³ that, so long as D_N is a decreasing function of N , then it matters little to the final aggregate structure what actual value the diffusion coefficient takes.) So, Eq. (5) is a simple but realistic way of allowing for *intra*-aggregate hydrodynamic effects; *inter*-aggregate hydrodynamic effects are neglected here.

At the start of a simulation run, particles are positioned at random subject to the condition $r > 2.4a$ for all pairs. Each simulation proceeds until all the particles have coagulated into a single 512-particle cluster. For potentials A and B , five separate runs were performed at each of the volume fractions $\phi = 0.05, 0.1, 0.15, 0.2, 0.25$, and 0.3 . Effective fractal dimensions D were calculated from plots of $\ln N$ against $\ln R_g$, where R_g is the radius of gyration ($R_g \sim N^{1/D}$).

The simulated aggregates are stringy on a long-length scale, but more compact on a short-length scale. Figure 2 shows one of the 512-particle clusters simulated with potential A at $\phi = 0.1$; it has a fractal dimension $D = 2.2$, and a $g(r)$ function as shown in Fig. 3(a). As ϕ increases, the aggregates become more space filling ($D \rightarrow 3$), and noticeably more structured at short range. An extrapolation to $\phi = 0$ gives $D = 2.0 \pm 0.1$ for potential A and $D = 1.9 \pm 0.1$ for potential B ; these fractal dimensions are similar to those obtained for reaction-limited aggregation and

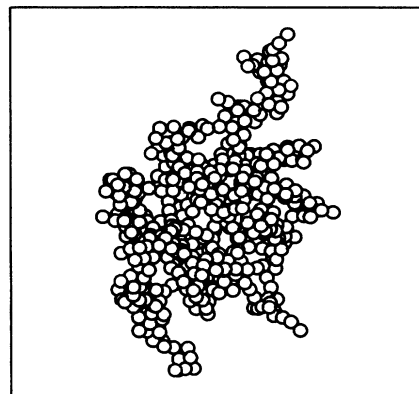


FIG. 2. A 512-particle cluster (potential A , $\phi = 0.1$).

diffusion-limited aggregation at high dilution^{3,4} ($D = 2.05$ and $D = 1.8$, respectively), and, within the statistical uncertainty, both values are close to that found experimentally with colloidal silica.^{5,8}

One complication in discussing fractal-type structure in nondilute systems is the formation of a gel state when aggregates get bigger than a certain average critical size. Using an analysis based on percolation theory,¹⁷ we have estimated that gelation sets in at $\phi \gtrsim 0.15$ for the 512-particle aggregates simulated here, which means that the final gel structures generated at the higher volume fractions, while heterogeneous and fractal on the short-to-

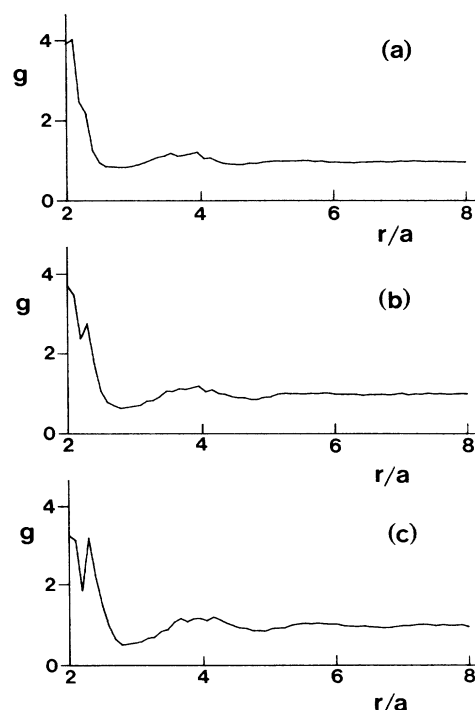


FIG. 3. Normalized $g(r)$ for final aggregates generated with potential A at (a) $\phi = 0.1$, (b) $\phi = 0.2$, and (c) $\phi = 0.3$.

TABLE I. Effective fractal dimension D (± 0.05) of aggregates as a function of particle volume fraction ϕ and colloidal potential (A or B).

ϕ	$D(A)$	$D(B)$
0.05	2.12	2.07
0.10	2.21	2.19
0.15	2.39	2.36
0.20	2.46	2.38
0.25	2.53	2.43
0.30	2.56	2.56

medium scale, are homogeneous on the macroscopic scale. Based on sets of just five runs at each volume fraction, the statistical data are not good enough, however, to discern any nonlinearity in the plots of $\ln N$ against $\ln R_g$ at high volume fraction which might be consistent with a crossover from pregelation to post gelation behavior. For consistency sake, therefore, particularly with respect to comparing results from the two potentials, we have calculated all values of D in Table I from analyses of clusters up to $N=512$, though it should be recognized that the smaller aggregates have more statistical weight as there are more of them. We stress that the fractal structure described here refers not to the large- N limit but only to a restricted range of radius: up to $20a$ for $\phi=0.05$, and only up to $12a$ for $\phi=0.3$.

In the $g(r)$ plots in Fig. 3, the sharp peak at $r/a=2$ (really a δ function) corresponds to pairs of particles in direct contact in the primary minimum. The fairly sharp peak at $r/a \approx 2.3$ corresponds to nonbonded pairs in the secondary minimum of potential A . The soft peak at $r/a \approx 4$ corresponds to the "second shell" of liquidlike structure familiar in Monte Carlo simulations of stable DLVO-type systems.² The features at $r/a \approx 2.3$ and $r/a \approx 4$ become stronger as ϕ increases, and at $\phi=0.3$ a "third shell" of liquidlike structure is clearly evident [Fig. 3(c)]. As particle concentration increases, the short-range structure of the aggregated colloid becomes more like that of the equivalent stable colloid (i.e., the system immediately prior to aggregation). Similar qualitative structural features in $g(r)$ to those in Fig. 3 have also been found¹⁸ in colloidal sediments simulated by single-particle deposition.

Figure 4 shows $g(r)$ for aggregates formed with potential B at $\phi=0.15$. In this case, apart from the sharp peak at $r/a=2$, there is little short-range structure. Comparison with Fig. 3 indicates that the colloidal aggregate structure at short range is indeed sensitive to the interactions acting between the particles before they stick permanently, in agreement with results from a preliminary

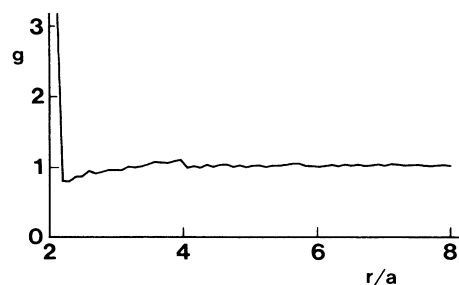


FIG. 4. Normalized $g(r)$ for final aggregates generated with potential B at $\phi=0.15$.

two-dimensional study.¹⁹ Such differences in short-range structure could have important implications for the mechanical properties of these aggregates (and gels formed therefrom), even though the longer-range structure, as measured by the effective fractal dimension (see Table I), is essentially the same for potentials A and B .

It would appear that the short-range structural features found with potential A are attributable to particles flocculating in the secondary minimum prior to irreversible aggregation. This allows clusters to "anneal" somewhat before the final configuration becomes "frozen in." Although the calculations reported here have been performed for large colloidal particles in which the secondary minimum of a few $k_B T$ arises from DLVO forces, we expect the same general behavior for any particles interacting with potentials of qualitatively similar form. With systems of small particles (e.g., the silica colloids of Schaefer and co-workers^{5,8}) where we would not expect a DLVO secondary minimum, it is possible that short-range structure like that indicated in Fig. 3 could arise through cluster rearrangement due to dissociation out of the primary minimum (peptization) on short time scales. This limited reversible aggregation could be limited on the longer time scale by excluded volume constraints or direct chemical bond formation between particle surfaces. Where the particles have some time to adopt an "equilibrium" structure before coagulation, we can say that the resulting aggregate structure is to some extent thermodynamically determined; otherwise, as here with potential B , it is kinetically determined. (The limiting form of thermodynamically determined behavior is the slow process of aggregation into a crystalline structure having long-range as well as short-range order.²⁰) These arguments are consistent with the recently reported x-ray results⁹ for aggregated gold colloids showing that the short-range structure as measured by $g(r)$ is dependent on whether coagulation occurs fast or slow. Light-scattering measurements of the initial coagulation behavior of polystyrene latex particles²¹ also lead to similar conclusions.

* Author to whom all correspondence should be addressed.

¹E. Dickinson, in *Colloid Science*, Specialist Periodical Report, edited by D. H. Everett (Royal Society of Chemistry, London, 1983), Vol. 4, p. 150.

²W. van Meegen and I. Snook, *Adv. Colloid Interface Sci.* **21**, 119 (1984).

³P. Meakin, *Phys. Rev. Lett.* **51**, 1119 (1983); *J. Colloid Interface Sci.* **102**, 491 (1984).

- ⁴M. Kolb, R. Botet, and R. Jullien, *Phys. Rev. Lett.* **51**, 1123 (1983); R. Jullien, M. Kolb, and R. Botet, *J. Phys. (Paris) Lett.* **45**, L211 (1984).
- ⁵D. W. Schaefer, J. E. Martin, P. Wiltzius, and D. S. Cannell, *Phys. Rev. Lett.* **52**, 2371 (1984).
- ⁶D. A. Weitz and M. Oliveria, *Phys. Rev. Lett.* **52**, 1433 (1984); D. A. Weitz, J. S. Huang, M. Y. Lin, and J. Sung, *ibid.* **54**, 1416 (1985).
- ⁷H. J. Herrmann, *Phys. Rep.* **136**, 153 (1986).
- ⁸D. W. Schaefer and K. D. Keefer, *Phys. Rev. Lett.* **56**, 2199 (1986); in *Fractals in Physics*, edited by L. Pietronero and E. Tosatti (North-Holland, Amsterdam, 1986), p. 39.
- ⁹P. Dimon, S. K. Sinha, D. A. Weitz, C. R. Safinya, G. S. Smith, W. A. Varady, and H. M. Lindsay, *Phys. Rev. Lett.* **57**, 595 (1986).
- ¹⁰E. J. W. Verwey and J. Th. G. Overbeek, *Theory of Stability of Lyophobic Colloids* (Elsevier, Amsterdam, 1948).
- ¹¹J. Mahanty and B. W. Ninham, *Dispersion Forces* (Academic, London, 1976).
- ¹²D. L. Ermak and J. A. McCammon, *J. Chem. Phys.* **69**, 1352 (1978).
- ¹³J. Bacon, E. Dickinson, and R. Parker, *Faraday Discuss. Chem. Soc.* **76**, 165 (1983).
- ¹⁴E. Dickinson, S. A. Allison, and J. A. McCammon, *J. Chem. Soc. Faraday Trans. 2*, **81**, 591 (1985).
- ¹⁵P. Meakin, Z.-Y. Chen, and J. M. Deutch, *J. Chem. Phys.* **82**, 3786 (1985).
- ¹⁶W. Hess, H. L. Frisch, and R. Klein, *Z. Phys. B* **64**, 65 (1986).
- ¹⁷S. A. Safran, I. Webman, and G. S. Grest, *Phys. Rev. A* **32**, 506 (1985).
- ¹⁸G. C. Ansell and E. Dickinson, *J. Chem. Phys.* **85**, 4079 (1986).
- ¹⁹G. C. Ansell and E. Dickinson, *Chem. Phys. Lett.* **122**, 594 (1985).
- ²⁰G. Y. Onoda, *Phys. Rev. Lett.* **55**, 226 (1985).
- ²¹D. Giles and A. Lips, *J. Chem. Soc. Faraday Trans. 2*, **74**, 733 (1978).